

Intracluster cyclization reaction producing a benzene derivative: photoionization mass spectrometric study of alkali metal–methyl propiolate clusters

Hironori Tsunoyama, Keijiro Ohshimo, Fuminori Misaizu*, Koichi Ohno¹

*Department of Chemistry, Graduate School of Science, Tohoku University, Aramaki, Aoba-ku,
Sendai 980-8578, Japan*

Received 19 June 2003; accepted 13 November 2003

Abstract

Size-dependent stability and intracluster reactions have been investigated by photoionization mass spectrometry for alkali metal (M; Li, Na, and K)–methyl propiolate (MP; HC≡CCOOCH₃) molecules clusters. In the photoionization mass spectra, the intensities of M⁺(MP)₃ ions (M=Na and K) were unexpectedly high, whereas no intensity anomaly was observed in Li⁺(MP)_n mass spectrum. The intensity anomaly can be explained by intracluster cyclization reaction induced by electron transfer from the metal atom and resulting a stable benzene derivative formation. Ion intensities of M⁺(MP)_n(H₂O) relative to M⁺(MP)_n have a minimum at $n = 3$ in Na and K systems. This result is owing to evaporation of water and/or MP molecules following exothermic cyclization reaction. Fragment ions with a loss of CH₂ were also observed predominantly from M(MP)₂ in all metal systems. These ions are expected to be produced by hydrolysis in M(MP)_n(H₂O) clusters producing a HC≡CCOOH molecule. The difference between lithium and other alkali metals is due to the rigidity of clusters with respect to deformation into geometry leading to the polymerization reaction.

© 2003 Elsevier B.V. All rights reserved.

Keywords: Polymerization; Cyclization; Intracluster reaction; Photoionization; Alkali metal

1. Introduction

Anionic polymerization reaction has been investigated for several decades as a method to obtain various useful materials [1,2]. It has been established that strong bases initiate anionic polymerization of vinyl compounds that bear electron-withdrawing substituents, such as cyano (CN) and carboxyl (CO₂R) groups. Electron transfer from strong bases, such as alkali metals and alkyllithium molecules, bring out a cleavage of the C=C double bond in the vinyl monomer. Thus, the contact ion pair of a negative ion of vinyl molecule and its counterion is expected to be produced in the initial step of polymerization. The ion pair is subsequently separated as a result of solvation. The carbanion

then reacts with another monomer to produce a carbanion with a longer chain as a propagating species. In several cases, some side reactions and electron transfer back to initiator terminate the reaction. The polymerization of acetylene derivatives have also been studied extensively in the past several decade in relation to conducting polymers [3]. Acetylene derivatives having electron-withdrawing groups are also known to be polymerized by anionic polymerization reaction. The reaction producing benzene derivatives from acetylene like molecules has also been studied, in which special metal complexes have been used as catalysts [3].

Intracluster ionic oligomerization is regarded as a microscopic model of initial step in polymerization in the condensed phase. Intracluster reactions for cluster cations [4–23] and anions [24–33] have been observed during the investigation of cationic and anionic polymerizations. Garvey and co-workers studied intracluster cationic polymerization in acetylene clusters [4], and in

* Corresponding author. Tel.: +81-222176577; fax: +81-222176580.

E-mail addresses: misaizu@qpcrkk.chem.tohoku.ac.jp (F. Misaizu), ohnok@qpcrkk.chem.tohoku.ac.jp (K. Ohno).

¹ Co-corresponding author.

acetylene–acetone heteroclusters [5]. In the mass spectra of acetylene and methylacetylene cluster ions, magic number behavior (intensity anomaly) at $n = 3$ was observed, and this behavior was explained by intracuster cyclization to produce benzene derivatives [4]. In the mass spectra of acetylene–acetone heterocluster cations $(C_2H_2)_n(C_3H_6O)_m^+$ and $(C_2H_2)_n(C_2H_3O)_m^+$ ion series were found and magic number behavior at $n = 2$ was observed in both clusters. This behavior was explained by the production of covalently bonded cyclic molecular ions $C_7H_{10}O^+$ and $C_6H_7O^+$. The acetylene cyclotrimerization was also recently studied on small MgO-supported Pd_n ($1 \leq n \leq 30$) clusters [34–37]. From these studies Pd atom on MgO (100) is found as a catalyst in selective benzene production from acetylene polymerization. As for anionic polymerization Kondow and co-workers have extensively studied reactions in cluster negative ions of acrylonitrile (AN) molecules and its derivatives [24–32]. In AN cluster negative ions intracuster oligomerization producing cyclohexane derivative was confirmed by the results of photodissociation, collision-induced dissociation, and photoelectron spectroscopy [24–28].

We previously reported intracuster anionic oligomerization in neutral clusters of alkali metal–vinyl molecules [38–42]. In these studies, clusters of an alkali metal atom ($M = Li, Na, \text{ and } K$) with some vinyl compounds ($VC = AN, \text{ acrylic ester, methacrylic ester, and methyl vinyl ketone}$) were examined by photoionization mass spectrometry. In these $M(VC)_n$ clusters, magic number behavior at $n = 3$ was commonly observed in photoionization mass spectra. This behavior was explained by formation of cyclohexane derivatives resulting from the anionic oligomerization initiated by electron transfer from alkali atom. In $M-AN$ clusters, the cyclohexane ring formation was confirmed by size distribution of metastable dissociation from $K^+(AN)_n$ photons [38], photodissociation of neutral clusters [39], and also by photoelectron spectroscopy of negative ion clusters [42].

In the present paper, we have investigated clusters containing alkali metal atom ($M = Li, Na, \text{ and } K$) and methyl propiolate molecules (MP; $HC\equiv CCOOCH_3$) by photoionization mass spectrometry. This molecule is a methyl ester of acetylene carboxylic acid, thus it can be compared with the methyl ester of ethylene carboxylic acid, i.e., methyl acrylate, $H_2C=CHCOOCH_3$, which have been studied by the authors' group [40]. Intracuster oligomerization reaction caused by electron transfer from metal atoms to molecules was discussed from size distributions observed in the mass spectra. Specific size distribution of cluster ions with one water molecule observed in the case of K and Na systems was also examined. The differences in observed features between alkali metal atoms were also discussed based on the results of quantum chemical density functional theory (DFT) calculations.

2. Experimental

Details of the experimental setup have been described in previous publications [38]. Briefly, the system is composed of three-stage differentially evacuated chambers which contain a cluster source and an angular type reflectron time-of-flight mass spectrometer (TOF-MS). Clusters of an alkali metal atom and MP molecules, $M(MP)_n$ ($M = Li, Na, \text{ and } K$), were generated by a pickup source [38–45] with a combination of laser vaporization and pulsed supersonic expansion. After being collimated with a conical skimmer the neutral clusters were ionized in an acceleration region of TOF-MS by irradiation with a laser beam. Nascently produced ions in laser vaporization source were repelled by static electric fields applied to the acceleration region. Frequency-doubled output of a dye laser (Spectra-Physics, PDL-2 and Inrad, Autotracker III) pumped by Nd:YAG laser (Spectra-Physics, GCR-150-10) was used as a photoionization light source. In order to avoid multiphoton ionization processes the laser fluence was kept under 4 mJ/cm^2 throughout measurements. Photoionized clusters were then accelerated to $\sim 3.0 \text{ keV}$ by electric fields between acceleration electrodes. After traveling a field-free drift region these ions were reflected back to an ion detector by reflection electrodes. The mass-separated ions were detected by a dual microchannel plate (MCP, Hamamatsu Photonics, F1552-21S) and output signals were stored by a digital oscilloscope (LeCroy, 9344C).

Along with the above measurements mass spectra of $K^+(MP)_n$ ions nascently produced in the cluster source were also measured. $K^+(MP)_n$ ions were generated by ion–molecule reaction between vaporized K^+ ions and MP clusters formed in the expansion region of free jet. These ions were accelerated to $\sim 1 \text{ keV}$ by pulsed electric fields generated by high voltage pulse generators (DEI, GRX-1.5K-E).

The sample rods of sodium and potassium were made from a lump under nitrogen atmosphere in a vacuum-drybox to avoid reactions with water in the air. The lithium rod was made in the same way under argon atmosphere in order to avoid reactions with nitrogen and water. The MP sample (Aldrich, 99%) was used without further purification.

3. Calculation

We performed quantum chemical calculations for a free MP molecule and $M(MP)$ ($M = Li, Na, \text{ and } K$) 1:1 complexes in order to examine the possibility of electron transfer and intracuster reaction. All calculations were carried out by using a DFT program of the Gaussian98 package [46]. The B3LYP functional [47] was utilized in these calculations in conjunction with 6-311 + G(d) basis sets for H, C, O, Li, and Na and 6-311G(d) basis set for K. The charge distributions of 1:1 complexes were also estimated using natural population analysis [48].

4. Results

4.1. Photoionization mass spectra of $M(\text{MP})_n$ ($M = \text{Li}, \text{Na}, \text{and K}$)

Typical photoionization mass spectrum of $\text{Li}(\text{MP})_n$ obtained by 5.64 eV laser irradiation is shown in Fig. 1a. In this figure a series of $\text{Li}^+(\text{MP})_n$ cluster ions is predominantly observed. In addition, several side peaks assignable to $\text{Li}^+(\text{MP})_n(\text{H}_2\text{O})_m$ are also detected, which are due to water impurity in methyl propiolate sample. Intensities of these hydrated cluster ions are found to increase with the number of n (MP molecules). Furthermore, fragment ion peaks assignable to a loss of CH_2 from $\text{Li}^+(\text{MP})_n$ is observed almost exclusively at $n = 2$. We also measured the photoionization mass spectra of Na–MP and K–MP as shown in Fig. 1b and c, respectively. As observed in $\text{Li}(\text{MP})_n$ clusters $\text{Na}^+(\text{MP})_n$ ion series is predominant with several side peaks assignable to $\text{Na}^+(\text{MP})_n(\text{H}_2\text{O})_m$. The fragment ion with a loss of CH_2 is also more pronouncedly detected for $n = 2$ than those of other cluster sizes. Similar features observed for Li–MP and Na–MP clusters are also obtained in case of K–MP system. In addition hydrated ion with $n = 3$, $\text{K}^+(\text{MP})_3(\text{H}_2\text{O})$, was more weakly observed than adjacent n values.

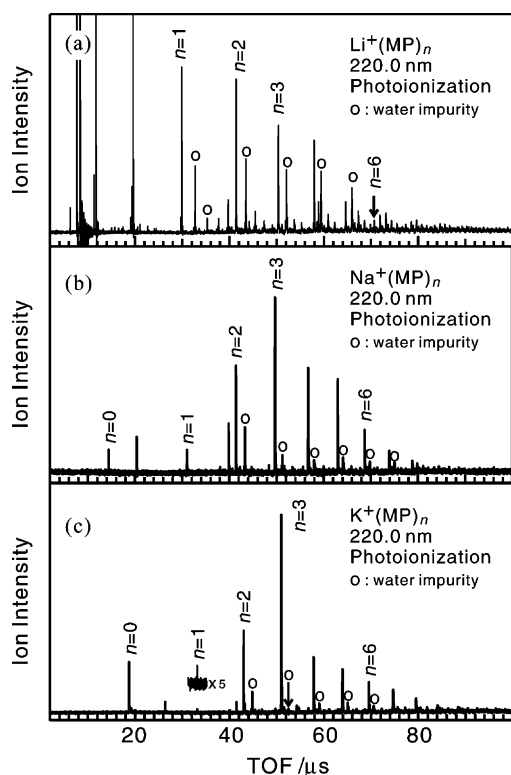


Fig. 1. Typical photoionization mass spectra of (a) $\text{Li}(\text{MP})_n$, (b) $\text{Na}(\text{MP})_n$ and (c) $\text{K}(\text{MP})_n$, with ionization energy of 5.56 eV. Series of $\text{M}^+(\text{MP})_n(\text{H}_2\text{O})_m$ are denoted by circles. A left-hand side peak of $n = 2$ in each mass spectrum indicates a fragment ion with loss of CH_2 from $\text{M}(\text{MP})_2$.

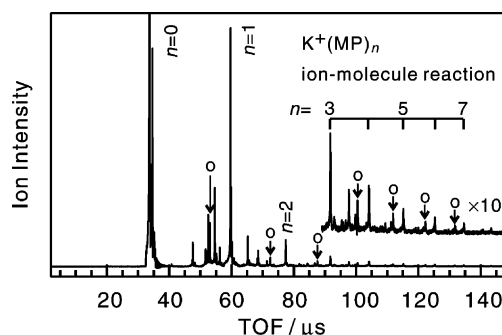


Fig. 2. Typical mass spectrum of $\text{K}^+(\text{MP})_n$ produced by ion–molecule reaction in the cluster source. Ions indicated by circles are assigned to be fragment ions with a loss of C_2H_2 from $\text{K}^+(\text{MP})_n$.

As noted above, some features are observed commonly for all metal systems. In particular fragment ion peaks assignable to the loss of CH_2 are commonly observed from $n = 2$ in all mass spectra (Fig. 1a–c). In contrast, the size distribution of $\text{M}^+(\text{MP})_n$ shows different tendency between lithium and other alkali metal atom systems. In the mass spectra of $\text{Na}^+(\text{MP})_n$ and $\text{K}^+(\text{MP})_n$ (Fig. 1b and c) the ions for $n = 3$ are prominently observed with respect to adjacent n clusters, whereas there is no evidence for such intensity enhancement in the mass spectrum of $\text{Li}^+(\text{MP})_n$. Furthermore, this intensity enhancement at $n = 3$ in Na and K systems are found to be independent from the ionization laser wavelength between 4.66 and 5.64 eV.

We also measured a mass spectrum of $\text{K}^+(\text{MP})_n$ produced by ion–molecule (cluster) reactions in the cluster source, as shown in Fig. 2. Cluster ion series of $\text{K}^+(\text{MP})_n$ are predominant in the observed photoionization mass spectra whereas no peaks are assignable to $\text{K}^+(\text{MP})_n(\text{H}_2\text{O})_m$. The ion intensity of $\text{K}^+(\text{MP})_n$ monotonically decreases with increasing cluster size n in contrast to the size distribution of photoionized $\text{K}^+(\text{MP})_n$. Several ions are found in the mass range between K^+ and $\text{K}^+(\text{MP})$ although difficult to be assigned them. In addition fragment ions, which are assignable to a loss of C_2H_2 from $\text{K}^+(\text{MP})_n$ clusters are also observed for $n = 1$ –8.

4.2. Geometrical structures and electron distributions of $\text{M}(\text{MP})_n$ ($M = \text{Li}, \text{Na}, \text{and K}$)

In order to get insight into the possibility of intracluster electron transfer and anionic oligomerization we optimized the 1:1 complexes of metal atoms and monomers using DFT. First the obtained structures for a neutral molecule and a negative ion of MP are shown in Fig. 3a and b, respectively. Two different types of structural isomers (**I** and **II**) were obtained both for neutral and anion: relative position of OCH_3 and $\text{C}=\text{O}$ is symmetric in isomer **I** and anti-symmetric in isomer **II**. However, there are two significant differences between neutrals and anions. Both of the two neutral isomers have planar structures whereas the two

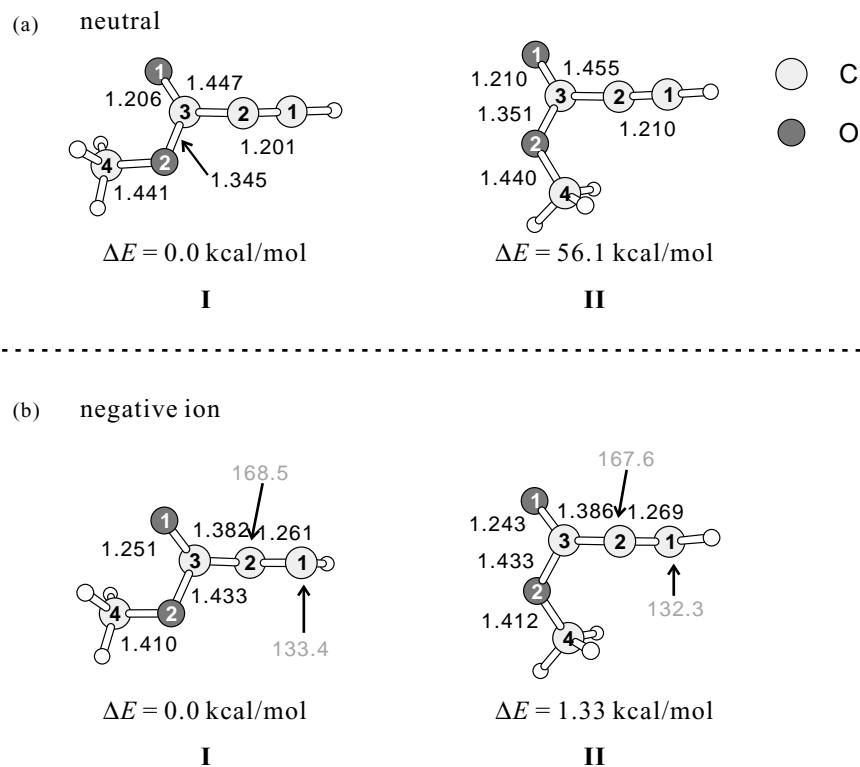


Fig. 3. Optimized structures of (a) neutral MP and (b) MP negative ion for two conformational isomers. Bond lengths and angles are shown in angstroms (Å) and degrees ($^{\circ}$), respectively. Energy difference between isomers **I** and **II** is shown as ΔE .

isomers of negative MP ion have bent structures in which $C\equiv C-H$ is out of the plane. On the other hand, isomer **I** is far more stable than **II** in neutral MP molecules while both isomers have comparable energies for anions, as indicated in Fig. 3. The structures obtained for M-MP 1:1 complexes ($M = Li, Na, \text{ and } K$) are shown in Fig. 4 and relative and binding energies between the metal atoms and the molecules are shown in Table 1. In addition, the natural charges of these complexes are shown in Table 2. In Na(MP) and K(MP) clusters five types of structural isomers (**1–5**) were obtained. In case of Li(MP) complex isomer **4** where Li atom would bound to the oxygen atom of $C=O$ group was not obtained. In all cases isomers **1** and **2** have almost the same total energy (within 3 kcal/mol) and they are more stable than isomers **3–5**. Therefore, we will discuss charge distributions and binding energies only for isomers **1** and **2** in all M-MP systems. In M(MP) isomers **1** and **2** ($M = Li, Na, \text{ and } K$) natural charges on the metal atom are estimated to be nearly unity. So the electron transfer from the metal atom to molecules equally occurs in all M-MP systems. Next we note differences between Li, Na, and K systems. In isomer **1** of Na(MP) and K(MP), binding energies between the metal atom and the MP molecule are 12.65 and 16.94 kcal/mol, respectively. In contrast to that the binding energy of Li(MP) isomer **1** is 32.27 kcal/mol, which is two times larger than those of Na(MP) and K(MP) complexes.

Table 1

Binding energies between alkali atom and MP molecule and relative energies with respect to most stable isomer **1** for M(MP) clusters ($M = Li, Na, \text{ and } K$)

Isomer ^a	Binding energy (kcal/mol)	Relative energy (kcal/mol)
Li(MP)		
1	32.27	0
2	31.04	-2.53
3	23.15	-9.12
5	29.59	-3.99
Na(MP)		
1	12.65	0
2	11.27	-2.68
3	4.30	-8.35
4	4.14	-8.51
5	7.88	-6.08
K(MP)		
1	16.94	0
2	15.79	-2.46
3	11.43	-5.51
4	4.42	-12.52
5	11.79	-6.46

Binding energies (ΔE) were estimated by the energy difference between complex (E_{complex}) and free alkali atom (E_{metal}) and free MP (for isomer **1**, E_{MP}), $\Delta E = -(E_{\text{complex}} - E_{\text{metal}} - E_{\text{MP}})$.

^a Isomers shown in Fig. 4.

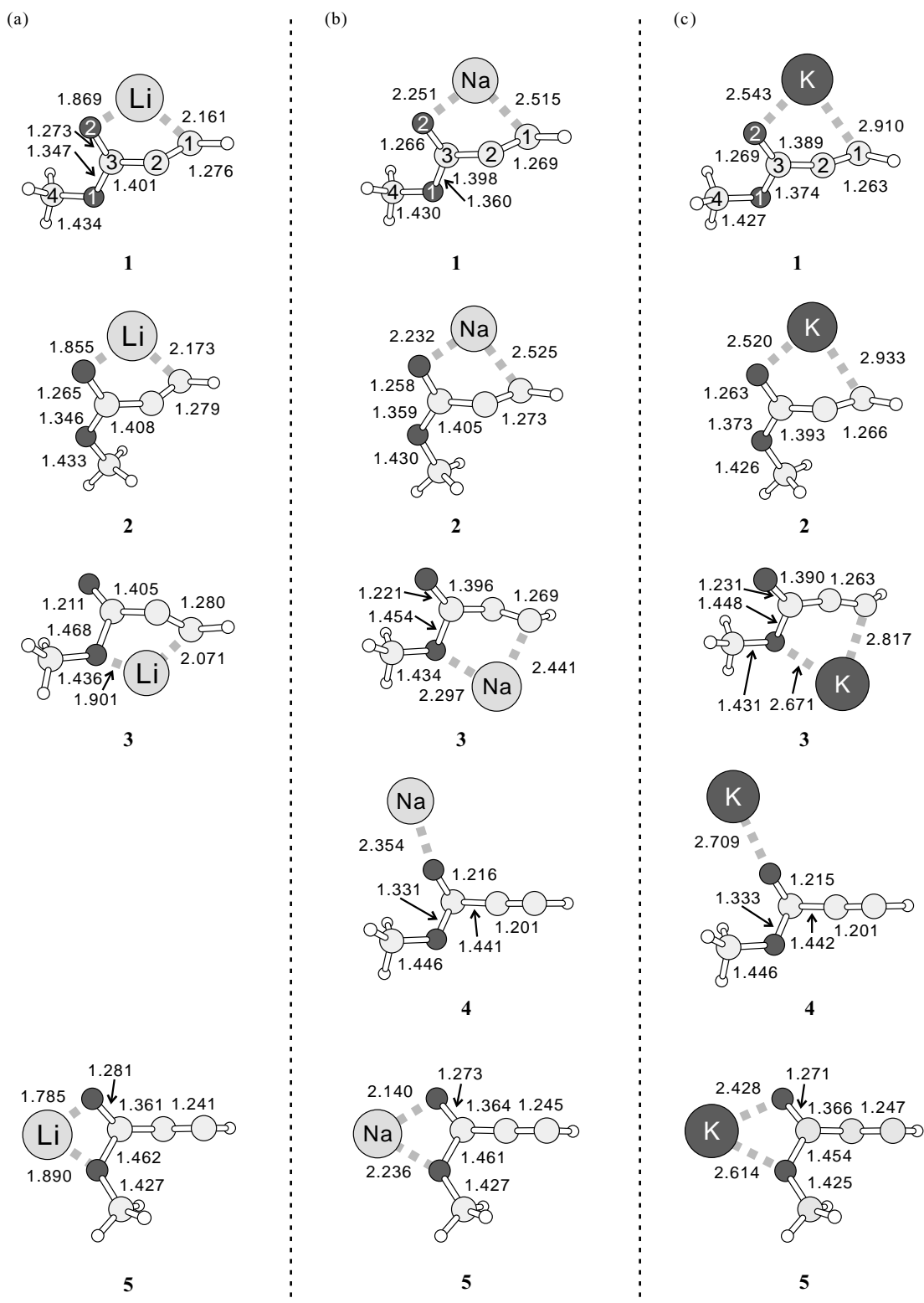


Fig. 4. Optimized structures of isomers in (a) Li(MP), (b) Na(MP), and (c) K(MP) 1:1 complexes. These isomers are classified into 1–5 according to the metal–MP bond.

Table 2
Natural charges of M(MP) (M = Li, Na, and K) at optimized structures

Isomer ^a	M	C1	C2	C3	O1	O2
MP		-0.13	-0.11	+0.72	-0.54	-0.52
Li(MP)						
1	+0.90	-0.49	-0.24	+0.61	-0.79	-0.52
2	+0.90	-0.48	-0.31	+0.63	-0.76	-0.52
3	+0.89	-0.53	-0.24	+0.63	-0.58	-0.71
5	+0.94	-0.24	-0.23	+0.54	-0.84	-0.71
Na(MP)						
1	+0.88	-0.48	-0.22	+0.60	-0.77	-0.54
2	+0.89	-0.47	-0.28	-0.62	-0.74	-0.53
3	+0.87	-0.50	-0.22	+0.61	-0.61	-0.68
4	+0.01	-0.10	-0.13	+0.74	-0.64	-0.50
5	+0.95	-0.27	-0.24	+0.54	-0.81	-0.69
K(MP)						
1	+0.94	-0.46	-0.22	+0.57	-0.78	-0.55
2	+0.94	-0.45	-0.28	+0.58	-0.75	-0.55
3	+0.93	-0.48	-0.23	+0.55	-0.62	-0.66
4	+0.02	-0.10	-0.12	+0.74	-0.63	-0.50
5	+0.97	-0.29	-0.25	+0.55	-0.82	-0.68

The numbering of C1–C3 and O1–O2 are displayed in Fig. 3.

^a Isomers shown in Fig. 4.

5. Discussion

5.1. Origin of intensity enhancement of $M(MP)_3$ ($M = Na$ and K)

There are three factors determining size distribution in photoionization mass spectrum of the present metal–molecules cluster system, which were already discussed in the previous papers [38–41]: (1) relative abundance of neutral clusters reflecting size-dependent stability, (2) ionization efficiency of neutral clusters at given photon energy, and (3) evaporation processes after ionization. We obtained photoionization efficiency curves of $Na(MP)_n$ for $n = 1–4$ by changing the ionization photon energies between 4.43 and 4.96 eV as shown in Fig. 5, and determined ionization thresholds of these clusters as summarized in Table 3. Ionization thresholds for these clusters are found to be rather constant at 4.5 eV. Furthermore, intensity enhancement at $n = 3$ is constantly observed in such measurement with 4.66–5.64 eV ionizing laser energy. In the photoionization at 5.64 eV the ionization efficiency is expected to be almost independent of n because ionizing photon energy is far higher than ionization thresholds. On the other hand, intensity enhancement was still observed at 4.66 eV laser ionization, which is only about 0.1 eV above the thresholds of clusters with $n = 1–4$. Therefore, it is found that evap-

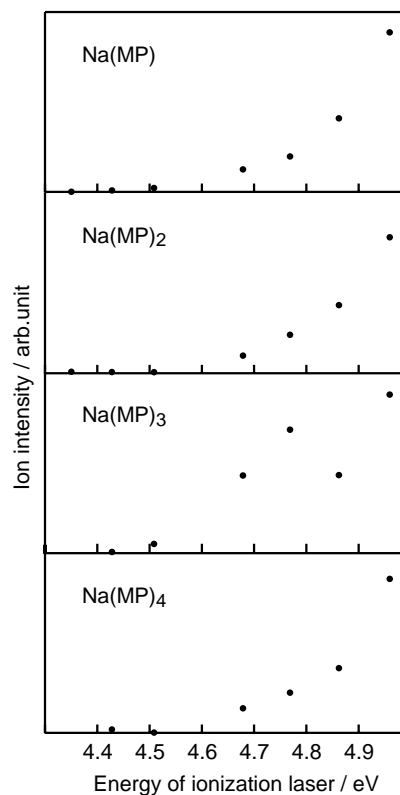


Fig. 5. Photoionization efficiency curves of $Na(MP)_n$ for $n = 1–4$.

oration processes do not also contribute sensitively to the intensity enhancement. If evaporation proceeds efficiently size distribution in the mass spectrum would be expected to reflect to the stabilities of cluster cations. However, no evidence of intensity enhancement has been found in the mass spectrum of nascently produced cluster ions (Fig. 2). After all the intensity enhancements observed in the photoionization mass spectra of $Na(MP)_n$ and $K(MP)_n$ are concluded to be due to the relative stability of neutral clusters (factor (1)).

Next we discuss the possible structures of neutral $M(MP)_n$ clusters. Clusters consisting of a metal atom and polar molecules have been mainly studied as microscopic model of solvation in electrolyte solution [43,44,49–52]. These clusters are supposed to have structures in which one metal atom or ion is surrounded by solvent molecules, thus their stabilities are dependent on the formation of solvation shells. The number of solvent molecules (m) in the first shell is expected to sensitively depend on the atomic radii of solvated metal atoms, for example, 1.86 and 2.27 Å for Na and K, respectively [53]. Therefore, the present result of the common intensity enhancement at $n = 3$ observed

Table 3
Determined ionization thresholds of $Na(MP)_n$ ($n = 1–4$)

	$n = 1$	$n = 2$	$n = 3$	$n = 4$
Ionization thresholds (eV)	4.54 ± 0.06	4.55 ± 0.07	4.49 ± 0.04	4.52 ± 0.05

for Na and K systems cannot be explained by the solvation structure. It is also possible that structures of clusters are concerned with new chemical bond formation as a result of intracuster reaction. Both in acrylonitrile (AN) cluster anion [24–33], $(\text{AN})_n^-$, and alkali metal–AN clusters [38,39], $\text{M}(\text{AN})_n$, magic number behavior at $n = 3k$ ($k = 1, 2, 3, \dots$) was observed. This behavior was concluded to be due to intracuster cyclization reaction producing cyclohexane derivatives (1,3,5-cyclohexanetricarbonitrile). Similar to this in alkali metal–acrylic ester and alkali metal–methacrylic ester clusters, we observed the same magic number behavior at $n = 3$ [40]. In alkali metal–vinyl molecules systems the stability of cyclized products sensitively depends on n due to ring strain. The product for $n = 3$ (cyclohexane derivatives) has lower ring strain than in case of other cluster sizes so the heat of intracuster oligomerization reaction for $n = 3$ is larger than in case of adjacent n clusters. However, in our present system the ring strain of the product for $n = 3$ is considered to be similar with $n = 4$ case because CCC bond angle of cyclooctatetraene (COT) and benzene have comparable values of 126° and 120° , respectively. In other words the cyclic product for $n = 3$ is not especially stable from the viewpoint of geometrical structure. The stability at this size can be explained by aromaticity of the cyclized products rather than their structures: The resonance energy of benzene molecule is known to be 37 kcal/mol, while in case of COT is only 5 kcal/mol [54]. In this system chain polyacetylene derivatives are also possible products of anionic polymerization as known in the bulk solution [3]. However, the stability of chain polymers is expected to change smoothly with a degree of polymerization (cluster size). For comparison, we also obtained a photoionization mass spectrum of aluminum atom–MP clusters as shown in Fig. 6. There is no evidence for intensity anomaly at $n = 3$ in $\text{Al}(\text{MP})_n$ clusters. This result is consistent with the prospect that the aluminum atom has so high ionization energy that the valence electron of the atom does not transfer to the MP molecules. Therefore, the magic number at $n = 3$ is a specific behavior in the clusters concerning with the microscopic model for anionic polymerization, such as alkali metal–methyl propiolate clusters. After all,

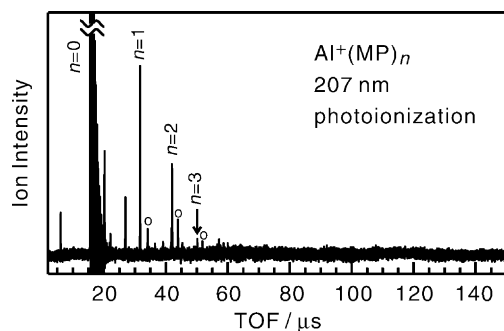
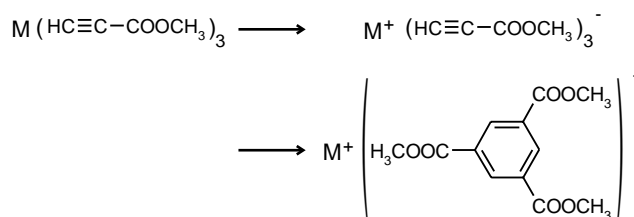


Fig. 6. Typical photoionization mass spectrum of $\text{Al}(\text{MP})_n$ with ionizing energy of 5.99 eV. Ion series of $\text{Al}^+(\text{MP})_n$ was mainly observed. Series of $\text{Al}^+(\text{MP})_n(\text{H}_2\text{O})_m$ are denoted by circles.



Scheme 1.

we concluded that the intensity enhancement at $n = 3$ is due to intracuster anionic oligomerization producing a benzene derivative (trimethyl 1,3,5-benzenetricarboxylate) (Scheme 1).

In the first step of this scheme an electron transfers from a metal atom to MP molecules, and then anionic polymerization is induced generating a benzene derivative in the second step. From the results of theoretical calculation on the natural population in 1:1 complexes mentioned in Section 4.2, it is expected that the electron transfer from the metal atom to $(\text{MP})_3$ is energetically favorable, although no data on the electron affinity of $(\text{MP})_3$ is available at the present. The polymerization step is highly exothermic, because the heat of production of trimethyl 1,3,5-benzenetricarboxylate from three MP molecules is estimated to be 181.8 kcal/mol at the B3LYP/3-21G level of theory. This energy is high enough to evaporate additional MP molecules from the clusters thus the evaporation processes after this reaction are expected to result the intensity enhancement at $n = 3$. Formation of this reaction product is also supported by comparison between experimentally determined ionization thresholds with those predicted by theoretical calculations. Ionization threshold of Na(trimethyl 1,3,5-benzenetricarboxylate) is estimated to be 4.25 eV, whereas that of unreacted van der Waals type $\text{Na}(\text{MP})_3$ is 3.52 eV, from B3LYP/3-21G level calculation². Ionization threshold from the experiment (4.49 eV) is in good agreement with the former value.

In the photoionization mass spectrum of $\text{Li}(\text{MP})_n$ the intensity enhancement at $n = 3$ was not observed in contrast to the Na–MP and K–MP systems. The study on photodissociation and mass spectrometry of $\text{Mg}^+(\text{AN})_n$, which has the same electron configuration as Na–AN system, no evidence was observed for magic number behavior at $n = 3$ although electron transfer from magnesium monocation to

² For structure optimization of unreacted $\text{Na}(\text{MP})_3$, we started optimization from a more symmetric structure where each Na–MP portion has a similar structure to the most stable isomer of $\text{Na}(\text{MP})$. We also optimized the structure of corresponding cation cluster starting from the neutral $\text{Na}(\text{MP})_3$. In case of reacted $\text{Na}(\text{MP})_3$ we found two isomers; (1) more symmetric structure in which sodium atom is located at on-top position of a benzene ring, (2) less symmetric structure where sodium atom lies near one of carbonyl oxygen of trimethyl 1,3,5-benzenetricarboxylate. We also obtained structures of cation complexes which are similar to neutral structures. We estimate ionization energy of reacted $\text{Na}(\text{MP})_3$ from (2) isomer which is 13.35 kcal/mol more stable than (1) isomer. More details will be published by H. Tsunoyama, F. Misaizu, and K. Ohno.

AN molecules in case of $n = 3$ cluster ion suggested by theoretical calculations. The difference between Mg^+ -AN and Na-AN systems was concluded to be due to the rigidity against deformation into a suitable geometry for polymerization reaction [55]. In order to induce intracuster cyclization reaction, each AN molecule should be reoriented to form new chemical bond and energy of this deformation are expected to be similar with binding energies between the metal atom and an AN molecule. Because the binding energy between Mg^+ and AN was estimated to be five times larger than between Na and AN the deformation necessary for the intracuster cyclization is thermodynamically much less favored in Mg^+ -AN system than in Na-AN system. In the present system, the binding energy between Li and MP molecule is two times larger than in Na-MP and K-MP systems, as shown in Table 1. Therefore, it is expected that the observed difference of intracuster cyclization between Li and other alkali atoms is due to this rigidity. In other words, the structural deformation before cyclization reaction occurs in Li-MP cluster more difficult than in other alkali metal systems. In addition intensity enhancement at $n = 3$ was not observed in MP negative ion clusters, $(\text{MP})_n^-$ [56]. So it is considered that alkali atom has also an important role not only as an electron donor but also as a catalyst.

5.2. Size distribution of water adduct clusters

In Fig. 1, cluster ions with one water molecule, $\text{M}^+(\text{MP})_n(\text{H}_2\text{O})$, were observed in all systems. We plotted intensity ratio between $\text{M}^+(\text{MP})_n$ and $\text{M}^+(\text{MP})_n(\text{H}_2\text{O})$ for $n = 1-7$ (Fig. 7). The ratios for Na-MP and K-MP systems are found to be especially weak at $n = 3$ whereas the ratio increases with n in Li-MP system. In the solvation-type $\text{M}(\text{MP})_n(\text{H}_2\text{O})$ clusters the relative abundance of $\text{M}(\text{MP})_n(\text{H}_2\text{O})$ is expected to depend smoothly on n because the abundance is determined by the concentration of water relative to MP in the sample gas and by the probability of addition of water to $\text{M}(\text{MP})_n$. The heat of intracuster cyclization reaction is high enough to support the evaporation of MP and water molecules. If these evaporation processes efficiently occur, it is expected that the intensity of $\text{M}(\text{MP})_3$ is enhanced rather than $\text{M}(\text{MP})_n$ ($n \geq 4$) and $\text{M}(\text{MP})_n(\text{H}_2\text{O})$ because the cyclized benzene derivative product of $(\text{MP})_3$ is inefficiently evaporated due to large binding energy. In Na-MP system, the cyclized product is presumed to exist in addition to solvation-type clusters so the intensity ratio of $\text{Na}^+(\text{MP})_3(\text{H}_2\text{O})/\text{Na}^+(\text{MP})_3$ is smaller than adjacent n as shown in Fig. 7b whereas the intensity of $\text{Na}^+(\text{MP})_3(\text{H}_2\text{O})$ is not specially weak in the photoionization mass spectrum (Fig. 1b). In K-MP system the existence of cyclized product is considered to decrease the ratio at $n = 3$ in Fig. 7c and the intensity of $\text{K}^+(\text{MP})_3(\text{H}_2\text{O})$ in the mass spectrum (Fig. 1c). Low intensity of $\text{K}^+(\text{MP})_3(\text{H}_2\text{O})$ suggests that the cyclization reaction occurs more efficiently in K-MP system than in other alkali metal-MP systems.

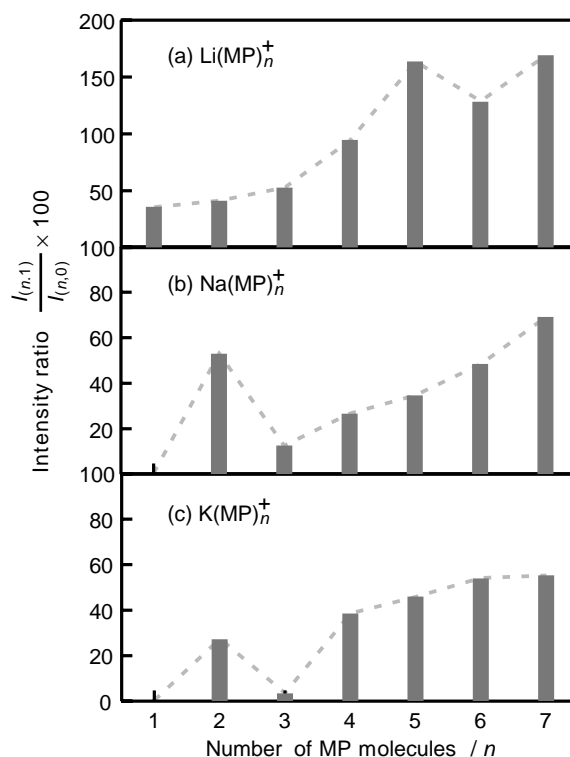


Fig. 7. Intensity ratio of $\text{M}(\text{MP})_n$ vs. $\text{M}(\text{MP})_n(\text{H}_2\text{O})$ are shown in percent for (a) Li-MP, (b) Na-MP, and (c) K-MP systems.

5.3. Formation of fragment ions assigned to a loss of CH_2 from $n = 2$

In all M-MP systems fragmented ion peaks with $m/z = m_a + 154$ (m_a : mass of alkali metal atoms), which is assignable to a loss of CH_2 from $\text{M}(\text{MP})_2$ are more prominently observed than in case of other cluster sizes. The most probable reaction to produce a fragment species with CH_2 loss from MP is hydrolysis of MP molecules because direct fragmentation of CH_2 from MP is highly endothermic. In contrast, no peaks for the loss of CH_2 from all cluster sizes are detected in the mass spectrum of $\text{K}^+(\text{MP})_n$ cluster ions produced by ion-molecule reaction. Therefore, the fragment ions are not produced by hydrolysis of MP sample in the reservoir before introducing into vacuum. In addition the size distribution of fragment ions produced by hydrolyzed MP molecules is expected to be almost independent of n if such reactions proceed in the liquid sample. Thus, the most probable reaction pathway is the hydrolysis in neutral $\text{M}(\text{MP})_n(\text{H}_2\text{O})$ clusters. The positive charge on C3 atom in MP (see Fig. 3) is considered to be indispensable to the reaction rate of the hydrolysis because hydrolysis is a nucleophilic substitution reaction on this atom. In $n = 2$ cluster the atomic charge on C3 is estimated to be +0.62, which is larger than that in $n = 1$ (+0.57) in K-MP system. Thus, we consider that the hydrolysis more efficiently occurs in case of $n = 2$ than in case of $n = 1$. The reaction rates for $n \geq 3$ clusters are considered to decrease due

to the geometrical structure, although more rigorous and systematic calculations on the geometry and stability are necessary.

Another possibility of the fragmentation is the reaction induced by the heat of cyclization reaction. For example, the fragment ion peaks with losses of HCN and H₂ from $n \geq 3$ were found to be produced by the heat of intracuster cyclization reaction in our previous study on M(AN)_n systems [38]. However, the stable fragmentation products with $m/z = m_a + 154$ from M(MP)₃ cannot be found in the present system although the heat of reaction in the present system is estimated to be high enough to induce the fragmentation, as discussed above. In addition the fragment ion peaks were also observed in Li–MP system whereas no evidence for intracuster cyclization was observed. Therefore, from the present observation we can expect that the fragmentation reaction proceeds independently from the cyclization reaction.

6. Conclusion

We have measured photoionization mass spectra of clusters containing an alkali metal atom (M = Li, Na, and K) and methyl propiolate (MP) molecules, M(MP)_n. The intensity enhancement at $n = 3$ was observed for M = Na and K, although there was no evidence for intensity enhancement in case of Li–MP system. This intensity enhancement can be attributed to intracuster cyclization reaction (anionic oligomerization) producing a benzene derivative induced by electron transfer from the alkali metal atom. In addition ion intensities of M⁺(MP)_n(H₂O) relative to M⁺(MP)_n have a minimum at $n = 3$ in Na and K systems whereas this feature was not observed in Li–MP systems. This intensity drop is explained by evaporation of water molecules from M(MP)_n(H₂O)_m induced by the heat of intracuster cyclization reaction. The heat of this cyclization can induce evaporation of water molecules and unreacted MP molecules, so that intensity of M(MP)₃ was enhanced in Na–MP and K–MP systems where intracuster cyclization reaction occurs. In Li–MP systems intensity enhancement at $n = 3$ and intensity drop of water adduct ion was not observed, in contrast to Na–MP and K–MP systems. This difference can be attributed to be due to higher deformation energy into the favorable geometry of the polymerization reaction. The Li–MP clusters have large binding energies between the metal atom and molecules, and as a result, reorientation of MP molecules to induce polymerization is expected to be inhibited. In contrast such reorientation may be possible in Na–MP and K–MP clusters because of smaller binding energies. Fragment ions assignable to a loss of CH₂ mainly from M⁺(MP)₂ were also observed in all M–MP systems. This fragmentation is explained by intracuster hydrolysis in M(MP)_n(H₂O), and size specificity of fragmentation is considered to reflect charge distributions and geometrical structures in M(MP)_n clusters.

Acknowledgements

The authors thank to the Computer Center of the Institute for Molecular Science for provision of the Fujitsu VPP5000 computer. This work has been supported in part by a Grant-in-Aid for Scientific Research from the Japanese Ministry of Education, Science, Sports and Culture. Financial support from Mitsubishi Foundation is also acknowledged. H.T. and K. Ohshimo are supported by the Research Fellowship of the Japan Society for the Promotion of Science for Young Scientists. Dr. Hajgato Balazs is also acknowledged for critical reading of the manuscript.

References

- [1] T.E. Hogen-Esh, J. Smid, Recent Advances in Anionic Polymerization, Elsevier, New York, 1987.
- [2] T. Tsuruta, K.F. O'Driscoll (Eds.), Structure and Mechanism in Vinyl Polymerization, Marcel Dekker, New York, 1969.
- [3] S. Patai (Ed.), Supplement C2: The Chemistry of Triple-Bonded Functional Groups, Wiley, Chichester, 1994.
- [4] M.T. Coolbaugh, S.G. Whitney, G. Vaidyanathan, J.F. Garvey, J. Phys. Chem. 96 (1992) 9139.
- [5] S.G. Whitney, M.T. Coolbaugh, G. Vaidyanathan, J.F. Garvey, J. Phys. Chem. 95 (1991) 9625.
- [6] J.F. Garvey, W.R. Peifer, M.T. Coolbaugh, Acc. Chem. Res. 24 (1991) 48, and references therein.
- [7] M.S. El-Shall, C. Marks, J. Phys. Chem. 95 (1991) 4932.
- [8] M.T. Coolbaugh, G. Vaidyanathan, W.R. Peifer, J.F. Garvey, J. Phys. Chem. 95 (1991) 8337.
- [9] M.T. Coolbaugh, J.F. Garvey, Chem. Soc. Rev. 21 (1992) 163.
- [10] B.C. Guo, A.W. Castleman Jr., J. Am. Chem. Soc. 114 (1992) 6152.
- [11] J.S. Brodbelt, C.-C. Liou, S. Maleknia, T.-Y. Lin, R.J. Lagow, J. Am. Chem. Soc. 115 (1993) 11069.
- [12] (a) J. Wang, G. Javahery, S. Petrie, D.K. Bohme, J. Am. Chem. Soc. 114 (1992) 9665; (b) J. Wang, G. Javahery, S. Petrie, A.C. Hopkinson, D.K. Bohme, Angew. Chem. Int. Ed. Engl. 33 (1994) 206.
- [13] G.M. Daly, M.S. El-Shall, J. Phys. Chem. 98 (1994) 696.
- [14] M.T. Coolbaugh, G. Vaidyanathan, J.F. Garvey, Int. Rev. Phys. Chem. 13 (1994) 1.
- [15] G.M. Daly, Y.B. Pithawalla, Z. Yu, M.S. El-Shall, Chem. Phys. Lett. 237 (1995) 97.
- [16] S.R. Desai, C.S. Feigerle, J.C. Miller, J. Phys. Chem. 99 (1995) 1786.
- [17] M.S. El-Shall, G.M. Daly, Z. Yu, M. Meot-Ner (Mautner), J. Am. Chem. Soc. 117 (1995) 7744.
- [18] M.Y. Lykty, T. Rycroft, J.F. Garvey, J. Phys. Chem. 1000 (1996) 6427.
- [19] M.S. El-Shall, Z. Yu, J. Am. Chem. Soc. 118 (1996) 13058.
- [20] Y.B. Pithawalla, J. Gao, Z. Yu, M.S. El-Shall, Macromolecules 29 (1996) 8558.
- [21] Q. Zhong, L. Poth, Z. Shi, J.V. Ford, A.W. Castleman Jr., J. Phys. Chem. B 101 (1997) 4203.
- [22] K. Hiraoka, T. Sugiyama, T. Kojima, J. Katsuragawa, S. Yamabe, Chem. Phys. Lett. 349 (2001) 313.
- [23] Y.B. Pithawalla, M. Meot-Ner, J. Gao, M.S. El-Shall, V.I. Baranov, D.K. Bohme, J. Phys. Chem. A 105 (2001) 3908.
- [24] Y. Fukuda, T. Tsukuda, A. Terasaki, T. Kondow, Chem. Phys. Lett. 242 (1995) 121.
- [25] M. Ichihashi, T. Tsukuda, S. Nonose, T. Kondow, J. Phys. Chem. 99 (1995) 17354.
- [26] Y. Fukuda, T. Tsukuda, A. Terasaki, T. Kondow, Chem. Phys. Lett. 260 (1996) 423.

- [27] T. Tsukuda, T. Kondow, C.E.H. Dessent, C.G. Bailey, M.A. Johnson, J.H. Hendricks, S.A. Lyapustina, K.H. Bowen, *Chem. Phys. Lett.* 269 (1997) 17.
- [28] Y. Fukuda, M. Ichihashi, A. Terasaki, T. Kondow, K. Osada, K. Narasaka, *J. Phys. Chem. A* 105 (2001) 7180.
- [29] T. Tsukuda, T. Kondow, *J. Chem. Phys.* 95 (1991) 6989.
- [30] T. Tsukuda, T. Kondow, *Chem. Phys. Lett.* 197 (1992) 438.
- [31] T. Tsukuda, T. Kondow, *J. Phys. Chem.* 96 (1992) 5671.
- [32] T. Tsukuda, A. Terasaki, T. Kondow, M.G. Scarton, C.E. Dessent, G.A. Bishea, M.A. Johnson, *Chem. Phys. Lett.* 201 (1993) 351.
- [33] T. Tsukuda, T. Kondow, *J. Am. Chem. Soc.* 116 (1994) 9555.
- [34] A. Sanchez, S. Abbet, U. Heiz, W.-D. Schneider, H. Häkkinen, R.N. Barnett, U. Landmann, *J. Phys. Chem. A* 203 (1999) 9573.
- [35] S. Abbet, A. Sanchez, U. Heiz, W.-D. Schneider, A.M. Ferrari, G. Pacchioni, N. Rösch, *J. Am. Chem. Soc.* 122 (2000) 3453.
- [36] S. Abbet, A. Sanchez, U. Heiz, W.-D. Schneider, A.M. Ferrari, G. Pacchioni, N. Rösch, *Surf. Sci.* 454–456 (2000) 984.
- [37] S. Abbet, A.M. Ferrari, L. Giordano, G. Pacchioni, H. Häkkinen, U. Landman, U. Heiz, *Surf. Sci.* 514 (2002) 249.
- [38] K. Ohshimo, F. Misaizu, K. Ohno, *J. Phys. Chem. A* 104 (2000) 765; K. Ohshimo, F. Misaizu, K. Ohno, *J. Chem. Phys.* 117 (2002) 5209.
- [39] K. Ohshimo, F. Misaizu, K. Ohno, *Eur. Phys. J. D* 16 (2001) 107.
- [40] (a) H. Tsunoyama, K. Ohshimo, F. Misaizu, K. Ohno, *J. Am. Chem. Soc.* 123 (2001) 683; (b) H. Tsunoyama, K. Ohshimo, F. Misaizu, K. Ohno, *J. Phys. Chem. A* 105 (2001) 9649.
- [41] K. Ohshimo, A. Furuya, H. Tsunoyama, F. Misaizu, K. Ohno, *Int. J. Mass Spectrom.* 216 (2002) 29.
- [42] K. Ohshimo, F. Misaizu, K. Ohno, *Eur. Phys. J. D* 24 (2003) 339.
- [43] C.P. Schulz, R. Haugstätter, H.U. Tittes, I.V. Hertel, *Phys. Rev. Lett.* 57 (1986) 1703.
- [44] C.P. Schulz, R. Haugstätter, H.U. Tittes, I.V. Hertel, *Z. Phys. D: At., Mol. Clusters* 10 (1988) 279.
- [45] F. Misaizu, M. Sanekata, K. Tsukamoto, K. Fuke, *J. Phys. Chem.* 96 (1992) 8259.
- [46] M.J. Frisch, G.W. Trucks, H.B. Schlegel, G.E. Scuseria, M.A. Robb, J.R. Cheeseman, V.G. Zakrzewski, J.A. Montgomery Jr., R.E. Stratmann, J.C. Burant, S. Dapprich, J.M. Millam, A.D. Daniels, K.N. Kudin, M.C. Strain, O. Farkas, J. Tomasi, V. Barone, M. Cossi, R. Cammi, B. Mennucci, C. Pomelli, C. Adamo, S. Clifford, J. Ochterski, G.A. Petersson, P.Y. Ayala, Q. Cui, K. Morokuma, P. Salvador, J.J. Dannenberg, D.K. Malick, A.D. Rabuck, K. Raghavachari, J.B. Foresman, J. Cioslowski, J.V. Ortiz, A.G. Baboul, B.B. Stefanov, G. Liu, A. Liashenko, P. Piskorz, I. Komaromi, R. Gomperts, R.L. Martin, D.J. Fox, T. Keith, M.A. Al-Laham, C.Y. Peng, A. Nanayakkara, M. Challacombe, P.M.W. Gill, B. Johnson, W. Chen, M.W. Wong, J.L. Andres, C. Gonzalez, M. Head-Gordon, E.S. Replogle, J.A. Pople, *Gaussian98, Revision A11*, Gaussian Inc., Pittsburgh, PA, 2001.
- [47] A.D. Becke, *J. Chem. Phys.* 98 (1993) 5648.
- [48] A.E. Reed, R.B. Weinstock, F. Weinhold, *J. Chem. Phys.* 83 (1985) 735.
- [49] C.P. Schulz, I.V. Hertel, in: H. Haberland (Ed.), *Clusters of Atoms and Molecules II*, Springer-Verlag, Berlin-Heidelberg, 1994.
- [50] K. Fuke, K. Hashimoto, S. Iwata, *Adv. Chem. Phys.* 110 (1999) 431, and references therein.
- [51] K. Ohshimo, H. Tsunoyama, Y. Yamakita, F. Misaizu, K. Ohno, *Chem. Phys. Lett.* 301 (1999) 356.
- [52] H. Tsunoyama, K. Ohshimo, Y. Yamakita, F. Misaizu, K. Ohno, *Chem. Phys. Lett.* 316 (2000) 442.
- [53] J. Emsley, *The Elements*, 3rd ed., Oxford University Press, New York, 1998.
- [54] L. Pauling, *The Nature of the Chemical Bond*, 3rd ed., Cornell University Press, New York, 1960.
- [55] A. Furuya, K. Ohshimo, H. Tsunoyama, F. Misaizu, K. Ohno, H. Watanabe, *J. Chem. Phys.* 118 (2003) 5456.
- [56] H. Tsunoyama, K. Ohshimo, F. Misaizu, K. Ohno, unpublished result.